J Solid State Electrochem (2010) 14:797–802
DOI 10.1007/s10008-009-0852-z

ORIGINAL PAPER

Influence of laser microfabrication on silicon electrochemical behavior in HF solution

Kestutis Juodkazis · Jurga Juodkazytė · Putinas Kalinauskas · Titas Gertus · Edgaras Jelmakas · Hiroaki Misawa · Saulius Juodkazis

Received: 19 December 2008 / Revised: 14 April 2009 / Accepted: 17 April 2009 / Published online: 12 May 2009

Abstract Influence of direct laser writing with femtosecond pulses on electrochemical etching of n-type low conductivity (>1,000 Ωcm) silicon is demonstrated. It has been shown that thermal 1-μm-thick SiO_2 layer on silicon surface can be used as a protective layer in the electrochemical etching process. It has been found that laser ablation changes not only the surface morphology and structure of silicon samples but also the character of their anodic etching in aqueous solution of hydrofluoric acid. Formation of microvoids and caverns of irregular shape has been observed at the laser-ablated sites. It is proposed that the change of silicon conductivity from n- to p-type takes place at the laser fabricated regions. Processes of Si anodic oxidation and electrochemical etching are discussed.

Keywords Laser microfabrication · Si electrochemical processes · HF solution

K. Juodkazis (✉) · J. Juodkazytė · P. Kalinauskas
Institute of Chemistry,
A. Goštauto 9,
Vilnius 01108, Lithuania
e-mail: kesjuod@ktl.mii.lt

T. Gertus
Altechna Co. Ltd.,
Konstitucijos av. 23,
Vilnius 08105, Lithuania

T. Gertus
Laser Research Center, Vilnius University,
Saulėtekio 10,
10223 Vilnius, Lithuania

E. Jelmakas
Institute of Materials Science and Applied Research,
Saulėtekio 9,
Vilnius 2040, Lithuania

H. Misawa · S. Juodkazis
Research Institute for Electronic Science, Hokkaido University,
N21W10 CRIS Bldg.,
Sapporo 001-0021, Japan

Introduction

Integration of photonic and electronic functionalities is a promising direction of future micro-devices. Three-dimensional structuring of crystalline semiconductor materials has a number of applications in the fields of microelectronics, photonics, micro-fluidics, fuel cells, super capacitors, bioassay, and microelectromechanical systems [1–3].

In the case of silicon, the combination of a direct laser writing by focused femtosecond pulses and electrochemical etching is promising for the pattern definition on the surface of sample. In this way, complex multistep lithographic procedures can be avoided. The surface etching conditions can be controlled electrochemically with high precision otherwise lacking in chemical wet etching. Electrochemical etching of silicon depends on many factors; very important among them is front and backside illumination [3–7]. Despite numerous studies, the mechanism of the electrochemical processes taking place on Si surface has not been fully clarified yet. Quite unambiguous and even contradictory are the interpretations of the anisotropic anodic etching of silicon during which porous Si with nano-/micro- and macropores with high aspect ratio is formed. In [8, 9], it has been demonstrated that after removal of surface oxide layer from Si with HF, the surface of silicon becomes covered with Si surface hydride ≡Si–H. On the basis of these results, Gerisher et al. [10] and other researchers [11, 12]

have formulated the concept of photochemical dissolution of silicon in HF. According to this concept, the surface of Si is predominantly H-terminated, i.e., covered with ≡Si–H hydride layer, which is the reason for silicon passivity in aqueous solutions. Si holes, which form under illumination, activate hydride layer, as a consequence of which stepwise replacement of H atoms with F atoms takes place, resulting in the formation of surface fluorides ≡SiF, $=SiF_2$, compounds HSiF3 and SiF4 and, eventually, soluble SiF_6^{2-} complex. According to [10–12], such replacement is possible because bond Si–F is much stronger than Si–H. After the sequence of such elementary surface reactions, the initial SiH state is recovered. Such fluoride-mediated mechanism of Si dissolution seems questionable, however, due to several reasons. First of all, almost no fluoride, i.e., just below 0.1 at.%, is found on Si electrode surface [11], whereas the surface coverage with H atoms makes about 10 at.% [11]. Consequently, since the silicon surface coverage with H atoms is not continuous, it cannot be the reason for silicon passivity in acid and neutral media as well as in HF solutions. In addition to this, it is known [13] that SiF_2, $HSiF_3$, and SiF_4 are gases, which are hydrolyzed in aqueous medium. The latter fact is not taken into consideration. Moreover, according to the above mechanism [11], oxidation of Si^{2+} to Si^{4+} proceeds with formation of gaseous H_2, which should inevitably block the formation of pores in the bulk of Si electrode.

The other opinion is that no passivation takes place and the overall anodic etching reaction is as follows [5]:

$$6HF + Si \rightarrow SiF_6^{2-} + H_2 + 4H^+ + 2e^-, \quad (1)$$

whereas anisotropic etching is described by:

$$2h^+ + 6HF + Si \rightarrow SiF_6^{2-} + H_2 + 4H^+, \quad (2)$$

which means that anodic oxidation of Si is possible only at those surface sites, which are accessible to holes.

Recent studies [14] have evidenced the formation of Si–O and Si–OH bonds in addition to Si–H ones on the surface of silicon during anisotropic etching in the solution of 0.05 M fluoride medium (pH3) within 0–0.6 V (vs. Ag/AgCl). Moreover, it has been shown that at $E \approx -0.3$ V, i.e., in the vicinity of open-circuit potential (OCP), the surface of silicon is clean from the above indicated species. Houbertz et al. [15] have demonstrated that while the surface of Si electrode is free from oxides in the cathodic range of potentials, i.e., at $E < E_{OCP} \approx -0.97$ V (Ag/AgCl in 40% NH_4F (pH8), a thin layer of oxides (1.0–1.5 ML) is already present on the surface within the double layer region, whereas in the range of anisotropic anodic etching [$E > 0$ V (Ag/AgCl)], the amount of oxygen on Si surface increases many times [16, 17]. Thus, disregarding of oxide formation during chemical or electrochemical oxidation of Si in HF solutions seems to be unjustified and cannot lead to thorough understanding of the processes taking place on Si electrode surface.

The aim of this study was to evaluate the influence of Si surface modification by laser microfabrication on the electrochemical behavior of silicon.

Experimental

Laser microfabrication

The pattern for electrochemical etching was defined on the surface of silicon using laser microfabrication setup (an integration solution by Altechna), which consisted of a femtosecond laser Pharos (Light Conversion), galvano scanners (GSI Group), and high-precision linear motor driven stages (Aerotech). The scanner control application software was used to control all laser fabrication routine. This setup allowed flexibly employing the direct laser writing by femtosecond pulses [18].

The laser-ablated pattern was a grating with the dislocation type defect at the center (hereinafter, a vortex grating). Such gratings are used to generate vortex beams upon transmission or diffraction and are required in a number of applications for specific intensity and polarization control of laser beams. Fine tuning of the pattern's depth is necessary for the precise definition of the phase changes upon transmission/reflection. The fabricated three-dimensional patterns on the surface can be further used for molding.

The high resistivity, $>10^3\,\Omega$cm, n-type silicon of a (100) surface plane (from Nilaco) was laser micro-patterning by surface ablation. The surface of samples was of a mirror finishing with or without a 1-μm-thick thermal oxide layer. Thickness of the Si samples was 0.5 mm.

Focusing of femtosecond Yb:KGW laser pulses of λ= 1,030-nm wavelength was carried out with a f=25-mm lens. The diameter of a laser beam was d=2 mm at full width at half-maximum. The average laser power was up to 2 W (on the sample) at a 50-kHz repetition rate and the pulse duration was 275 fs. The diameter of focal spot can be estimated for the Gaussian beam as $2w_0 = \frac{4\lambda}{\pi}\frac{f}{d} \simeq 16\ \mu m$ with axial length equal to the doubled Rayleigh length, $2z_R = \frac{8\lambda}{\pi}\left(\frac{f}{d}\right)^2 \simeq 410\mu m$. The width of the laser-ablated lines in the grating patterns was determined by multiline patterning and continuous scanning.

The threshold value of the surface structuring by ablation at these focusing conditions for a 50% overlapping between adjacent pulses corresponded to the 1.9 TW/cm^2 per pulse irradiance or 0.5 J/cm^2 per pulse fluence on thermally oxidized silicon. These values are slightly lower than the

threshold of silica ablation since the ablation of a buried silicon, which has approximately four times lower threshold, was responsible for the surface microstructuring. The depth of an ablation pattern was ~2–5 μm depending on the pulse energy and overlap of pulses, while the width of laser-ablated grooves ranged between 20 and 100 μm. The ablated surfaces had a thin, nanometer-thick native oxide, which was removed chemically within seconds in aqueous HF electrolyte used in our experiments.

Structural characterization of laser-fabricated and electrochemically etched surfaces was carried out by scanning electron microscopy (SEM) using a TM-1000 (Hitachi) tabletop microscope.

Electrochemical measurements

Electrochemical measurements and etching were controlled by a potentio-/galvanostat PGSTAT302 (Autolab, Eco Chemie). Electrochemical cell used for measurements is shown schematically in Fig. 1. The n-type Si plate with a native or thermal 1-μm-thick oxide layer was used as a working electrode. The surface area of Si exposed to electrolyte was 0.63 cm^2. The electric contact at the backside of working Si electrode was realized by mechanical contact of Au wire with a freshly scratched Si surface. Hydrogen electrode in the working solution was used as reference and the counter electrode was platinum-coated titanium. Potential values in the text refer to standard hydrogen electrode scale unless noted otherwise. The electrolyte was a 2 M aqueous solution of hydrofluoric acid (pH ≈ 3). Photo-activation was qualitatively tested using a standard incandescent lamp. The intensity of backside illumination of Si electrode was 0.5 W/cm^2 as measured by a LM2 power meter (Carl Zeiss, Jena, Germany). All experiments were carried out at room temperature.

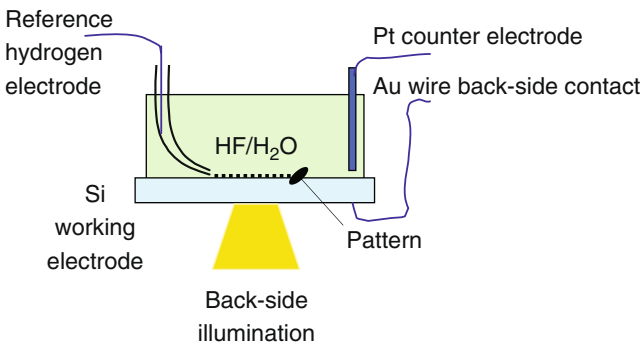

Fig. 1 Schematics of electrochemical cell for voltammetric measurements and etching of the pattern laser-ablated on the surface of Si. Electrical circuit was completed by a potentio-/galvanostat

Results and discussion

Electrochemical behavior of Si electrode in HF solution: role of illumination

Figure 2 shows cyclic voltammograms characterizing the electrochemical behavior of Si electrode in 2 M HF solution.

Open-circuit potential of Si electrode in this electrolyte was about −0.1 V. One can see that in the case of silicon surface covered with native oxide, the thickness of which should not exceed ~20 nm, the beginning of anodic process is observed at ~0.25 V. Cycling the potential within 0.25–3.0 V leads to a continuous increase in the rate of the anodic process (Fig. 2, curves 1–4). This may be related to activation of the electrode surface, i.e., to stepwise dissolution of native oxide layer, and the increase in the surface area of electrode taking part in electrochemical process. Backside illumination of the electrode increases the rate of anodic process considerably (Fig. 2, curve 5). The beginning of the anodic process at 0.25 V corresponds well to the values reported in the literature [3, 4, 14, 15].

The anodic range of potentials in Fig. 2 can be arbitrarily subdivided into two main zones: the first one from the beginning of anodic process up to ~0.75 V and the second at E>0.75 V. Such subdivision is more apparent in the case

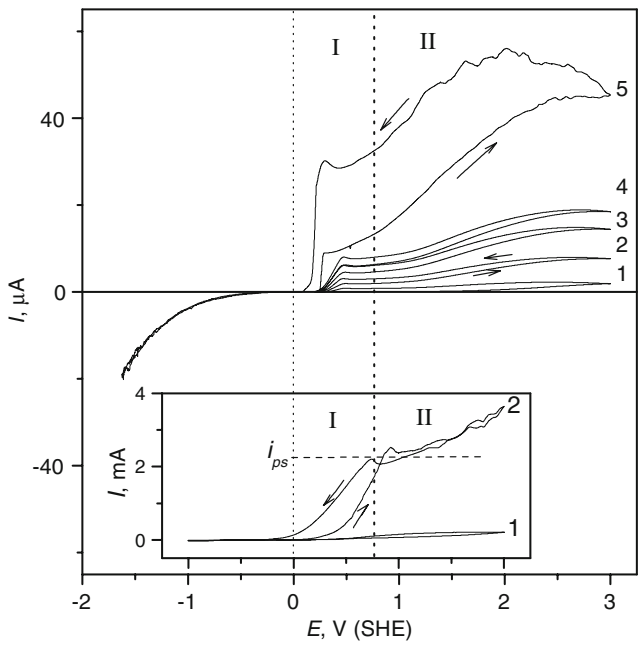

Fig. 2 Cyclic voltammograms of high resistivity n-type Si(100) electrode in 2 M HF: *1–4* without, *5* with backside illumination. *Inset*, cyclic voltammograms of the same Si electrode etched in concentrated HF for 30 s: *1*, *2* without and with backside illumination, respectively; 20 mV/s, 20 °C

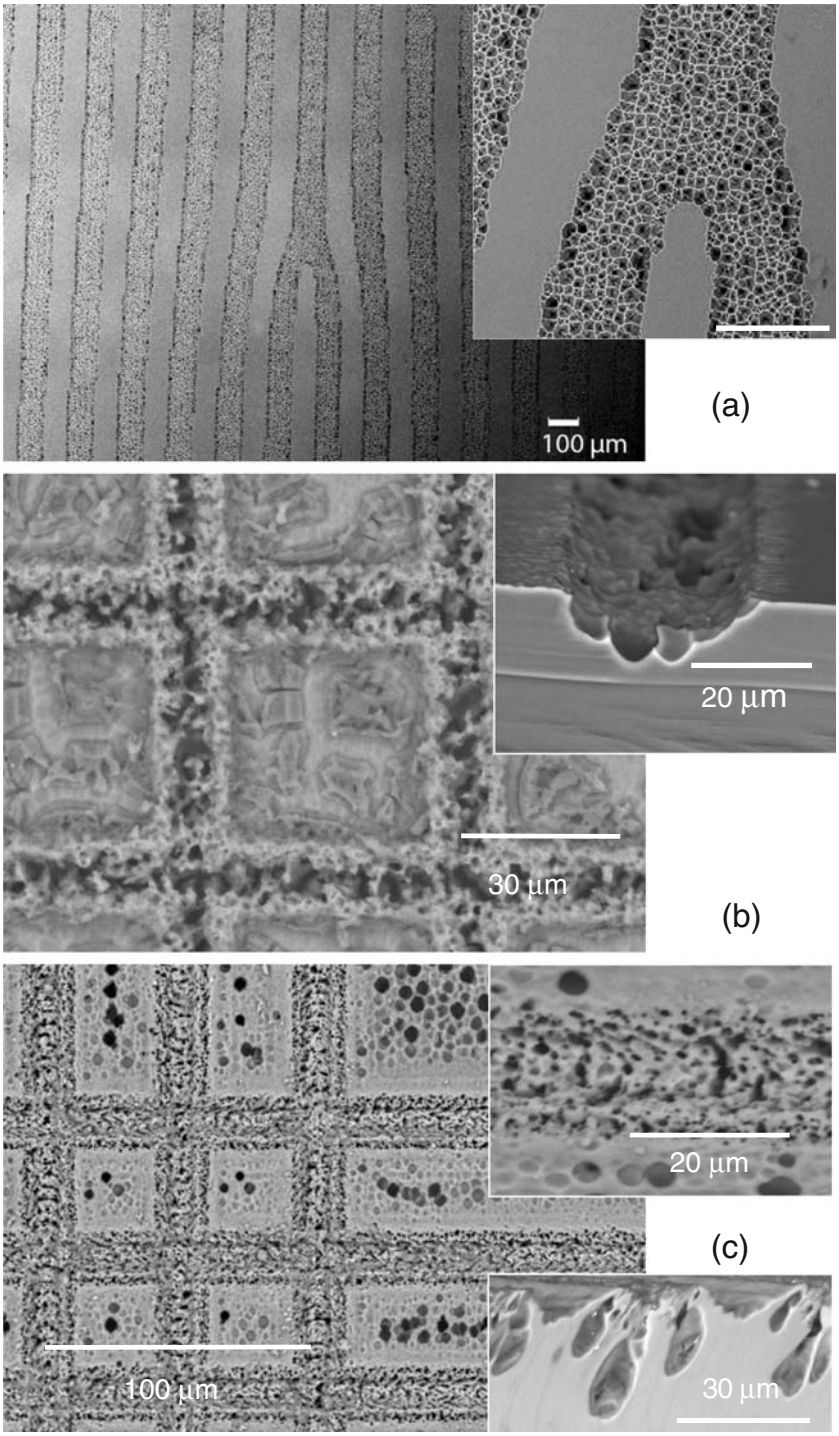

Fig. 3 Typical SEM images with detailed views of **a** the vortex grating: ablated pattern on silicon with thermal oxide layer after potentiostatic electrochemical etching at E=2.2 V, i_a≈1.5 mA, t_a=60 min; **b** laser-ablated trenches on silicon with thermal oxide layer after potentiostatic electrochemical etching at E=1.14 V, i_a=1.1–1.6 mA, t_a=30 min; **c** laser-ablated trenches on silicon with native oxide layer after galvanostatic electrochemical etching at i_a= 0.5 mA, E≈0.35 V, t_a=20 min. The laser power was 1.5 W (**a**), 1.0 and 3.0 W (*inset*) (**b**), and 1.0 W (**c**) at repetition rate of 50 kHz

shown in Fig. 4, curve 2. Lehman et al. [3, 5–7] have demonstrated that in the case of n-type Si, formation of porous silicon takes place within the first range. It has been shown [1–3, 5–7] that pores of various diameters with extremely high aspect ratio can be formed in n-type silicon by means of electrochemical etching in HF solutions under backside illumination provided that current density does not exceed the critical value of i_{ps} (porous silicon, ps; Fig. 2, the inset).

In the second range of potentials, uniform etching of the surface or the electropolishing takes place. It is known that within the first E range, formation of H_2 bubbles takes place on the electrode surface, but not on the inside of the pores [6], whereas at E> 0.75 V (II range), this process is

not observed. One can see from curve 5 (Fig. 2) and it is also known from the literature [11, 14] that the first anodic process is very facile and its slope dE/dln$i$ is close to RT/F, which is characteristic of reversible electrochemical process. When anodic current reaches its maximum value, the process slows down a little or reaches limitation. The rate of the process starts to increase again only in the second range of potentials. Thus, it is obvious that the mechanism of anodic process within the first and second E ranges differs and might be related to the gradual increase of oxidation state of Si. This conjecture is following straightforward thermodynamic arguments [13] and deserves further systematic studies.

The cathodic part of the voltammograms in Fig. 2 demonstrates that the main cathodic process, i.e., electrochemical formation of H_2 on the surface of silicon, is significantly hindered. The overvoltage of H_2 evolution is about 0.5 V at ~1 μA and 1.5 V at ~20 μA. The influence of front side illumination on the cathodic process is insignificant: It does not exceed ~1 μA at E=−1.5 V. In summary, the Si electrode under investigation exhibits passive behavior in HF solution within −0.5 to 0.3 V (Fig. 2).

Structural characterization of laser-ablated anodically etched silicon

Figure 3 summarizes the results of anodic etching of Si electrodes with various laser patterning in 2 M HF at different ranges of anodic potential (Fig. 2) under backside illumination. When etching was performed within the second range of anodic potentials (Fig. 3a) at E=2.2 V, i_a≈1.5 mA, t_a=60 min, the etching took place at the laser-ablated surface sites where one can see a random pattern of etching pits. Despite the long duration, about 1 h of electrochemical etching, formation of etching pits was not observed on the surface protected by the thermal oxide. This demonstrates that the thermal oxide served as a protective mask.

Similar result was observed for the sample shown in Fig. 3b where anodic etching was performed at milder conditions within the same E range (E=1.14 V, i_a=1.1–1.6 mA, t_a=30 min). Deepening and widening of laser-patterned trenches has been observed, as can be judged from the detailed view of sample cross-section. Though the layer of thermal SiO_2 was also affected by the etching, the rate of etching of oxide-protected and laser-ablated surface places was clearly different. As one can see from the detailed view in Fig. 3b, the etched pores are deep and have irregular cavern-type shape, in correspondence with earlier reports [16, 17].

In the case of Fig. 3c with detailed front and side views, both were electrochemically active laser-ablated places and the rest of the surface of n-type silicon covered with thin native oxide layer, which most likely very quickly dissolved in 2 M HF. The anodic etching in this case was performed under galvanostatic conditions within the first range of anodic potentials: i_a=0.5 mA, E≈0.35 V, t_a=60 min. In Fig. 3c, one can see a rather even distribution of small pores within laser-ablated trenches, whereas elsewhere, random pattern of micro- and macropores is seen, as could be expected in accordance with the literature [5]. Detailed cross-sectional view (Fig. 3c, lower inset) demonstrates the formation of caverns in silicon at laser-ablated places.

Figure 4 shows cyclic voltammograms of Si electrodes with thermal 1-μm-thick and native oxide layer, the surface of which was modified by laser ablation to form trenches of various widths. The voltammogram of laser-unmodified sample is shown as curve 1 for comparison. One can see that Si electrode with thermal 1-μm-thick oxide layer is completely passive in both cathodic and anodic ranges of potential. Thus, it is evident that the electrochemical response of sample (curve 2) is attributable to laser-ablated places of the surface only. Quite unexpectedly, however, laser-ablated Si electrodes exhibit electrochemical behavior characteristic for p-type silicon, as can be judged from a comparison with literature data [3], whereas the Si plate itself is of the n-type. Moreover, there is a definite hysteresis between positive- and negative-going parts of the voltammogram, which suggests that partial passivation of the electrode surface takes place within the second range of potentials. This was confirmed also by the voltammograms recorded after the anodic etching of Si surface where significant current oscillations are seen in the negative-going part of the curves (not shown in the figure). However, in the case of native SiO_2 oxide (Fig. 4, curve 3), the shape

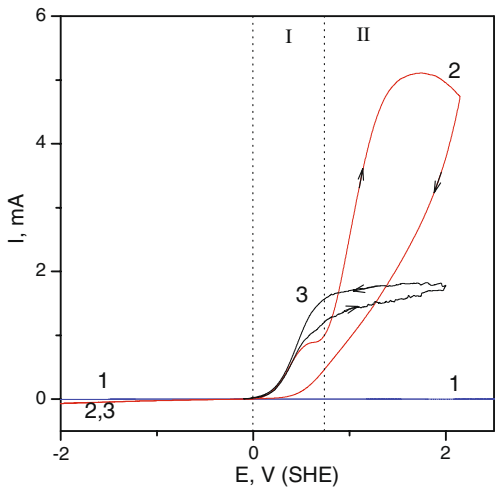

Fig. 4 Voltammograms of Si electrode in 4% HF under backside illumination, v=20 mV/s, 20°C: *1* with thermal 1-μm-thick oxide layer, *2* Si with thermal 1-μm-thick oxide layer and laser-ablated trenches, *3* with native oxide layer and laser-ablated trenches

of the voltammogram remained unchanged despite laser patterning (compare with Fig. 2, inset). This is attributable to the fact that not only laser-treated but also untreated surface of Si electrode is electrochemically active in the latter case.

The possible reason of the conductivity type change can be related to the defect generation in silicon. The regions near laser-ablated grooves were subjected to high temperatures, ultrafast thermal quenching, and defect generation [19, 20]. Laser ablation by ultrashort pulses when energy delivery and carrier excitation is shorter than thermalization times ~1 ps results in a full ionization (even a multiple ionization) of pre-surface regions [21]. Thermal quenching is also much faster when ultrashort sub-1-ps pulses are used for irradiation. As a result, a strong non-equilibrated defect generation is expected [22–24]. The vacancies usually act as acceptors in semiconductors [25]. It is likely that laser-ablated pattern shows a change in conductivity from n- to p-type due to defect formation.

It is noteworthy that reactivity of nanostructured materials can be much different from the solid-state phases. The enhanced chemical reactivity of shock-amorphized [26, 27] and pulverized nanostructured materials has been established; however, the exact mechanisms are not well understood [28–30]. Femtosecond laser microfabrication is well suited to form such non-equilibrium phases [31] of nanomaterials with much altered physical and chemical properties (e.g., in dielectrics [32–34]).

Conclusions

The experimental results demonstrate that modification of n-type Si surface with femtosecond laser pulses changes essentially the character of anodic etching. A considerable increase in the anodic etching rate was observed in the case of laser-treated samples. The character of voltammograms characteristic for p-type Si [3] was observed after laser microstructuring of an initially n-type low-conductivity silicon. It was demonstrated that a 1-μm-thick thermally grown oxide can be used as a mask which protects laser-unstructured regions of silicon in a 2 M HF electrolyte during electrochemical etching.

Acknowledgments Financial support by a 20070305-1 grant from Lithuanian "Mokslininku¸ sa¸jungos institutas" is gratefully acknowledged. SJ is thankful for support via a Grant-in-Aid from the Ministry of Education, Science, Sports, and Culture of Japan no. 19360322.

References

1. Kovacs GT, Maluf NI, Petersen KE (1998) Proc IEEE 86:1536
2. Klür MH, Sauermann A, Elsner CA, Thein KH, Dertinger SK (2006) Adv Mat 18:3135
3. Lehmann V (1996) Appl Surf Sci 106:402
4. Jakubowicz J (2007) Superlattices Microstruct 41:205
5. Lehman V, Föll H (1990) J Electrochem Soc 137:653
6. Lehman V (1993) J Electrochem Soc 140:2836
7. Lehman V, Grüning U (1997) Thin Solid Films 297:13
8. Ubara H, Imura T, Hiraki A (1984) Solid State Comm 50:673
9. Burrows VA, Chabal YJ, Higashi GS, Raghavachari K, Christman SB (1988) Appl Phys Lett 53:998
10. Gerisher H, Allongue P, Kieling VC (1993) Ber Bunsenges Phys Chem 97:753
11. Smith RL, Collins SD (1992) J Appl Phys 71:R1
12. Kolasinski KW (2003) Phys Chem Chem Phys 5:1270
13. Turova NY (1977) Spravochnye tablitsy po neorganicheskoi khimii. Khimiya, Leningrad
14. Outemzabet R, Cherkaoui M, Gabouze N, Ozanam F, Kesri N, Chazalviel JN (2006) J Electrochem Soc 153:C108
15. Houbertz R, Memmert U, Behm RJ (1998) Surf Sci 369:198
16. Foll H, Christophersen M, Carstensen J, Hasse G (2002) Mat Sci Eng Rep 39:93
17. Carstensen J, Christophersen M, Foll H (2000) Mat Sci Eng B 69:23
18. Juodkazis S, Matsuo S, Misawa H, Mizeikis V, Marcinkevicius A, Sun HB, Tokuda Y, Takahashi M, Yoko T, Nishii J (2002) J Appl Surf Sci 197–198:705
19. Gamaly EE, Juodkazis S, Nishimura K, Misawa H, Luther-Davies B, Hallo L, Nicolai P, Tikhonchuk V (2006) Phys Rev B 73:214101
20. Juodkazis S, Nishimura K, Tanaka S, Misawa H, Gamaly EE, Luther-Davies B, Hallo L, Nicolai P, Tikhonchuk V (2006) Phys Rev Lett 96:166101
21. Sundaram SK, Mazur E (2002) Nat Mater 1:217
22. Watanabe M, Juodkazis S, Sun HB, Matsuo S, Misawa H (1999) Phys Rev B 60:9959
23. Juodkazis S, Watanabe M, Sun HB, Matsuo S, Nishii J, Misawa H (2000) Appl Surf Sci 154:696
24. Eliseev P, Sun HB, Juodkazis S, Sugahara T, Sakai S, Misawa H (1999) Jpn J Appl Phys 38:L839
25. Böer KW (1990) Survey of semiconductor physics: electrons and other particles in bulk semiconductors, vol I. Van Nostrand Reinhold, NY, New York
26. Zel'dovich YB, Raizer YP (2002) Physics of shock waves and high-temperature hydrodynamic phenomena. Dover, Mineola, New York
27. Dremin AN (2000) Combust Explos Shock Waves 36:704
28. Johnson Q, Mitchell AC (1972) Phys Rev Lett 29:1369
29. Devine RAB, Dupree R, Farnan I, Capponi JJ (1987) Phys Rev B 35:2560
30. Belonoshko AB (1997) Science 275:955
31. McMillan PF (2005) Nat Mater 4:715
32. Juodkazis S, Nishimura K, Misawa H, Ebisui T, Waki R, Matsuo S, Okada T (2006) Adv Mater 18:1361
33. Juodkazis S, Misawa H (2008) Appl Phys A 93:857
34. Juodkazis S, Mizeikis V, Sudžius M, Misawa H, Kitamura K, Takekawa S, Gamaly EG, Krolikowski WZ, Rode AV (2008) Appl Phys A 93:129